Experiments on the penetration of an interface by buoyant thermals

By J. M. RICHARDS

Department of Meteorology, Imperial College, London*

(Received 3 January 1961 and in revised form 11 April 1961)

Isolated masses of a dense aqueous solution (i.e. thermals) were released at the surface of a freshwater layer overlying one of salt water. While the whole of a thermal remained in the upper layer, the equations $z = n_1 r$, $z^2 = k_1 t$, with $k_1 = C_1 n_1^{\frac{3}{2}} (Mg/\rho)^{\frac{1}{2}}$, were obeyed, where z is the distance travelled, $2r$ the width of the thermal, t the elapsed time, M the mass excess (the difference between the masses contained within and displaced by the thermal while in the upper layer), and ρ the density of the displaced fluid. n_1 was constant for any one thermal, but varied between thermals over the range 1·9 to 7·5. C_1 had roughly the same value (0·73) for all thermals.

The behaviour after the leading extremity of the thermal (the 'front') entered the lower layer depended on the value of the parameter $S = V\Delta\rho/M$, where $\Delta\rho$ is the density difference between the upper and lower layers and V is the volume of the thermal when the widest part is at the level of the discontinuity. It was found that $Y = 0$ if $S > \beta$ ('weak' thermals), and $Y = 0{\cdot}95 - \frac{1}{2}S$ if $0{\cdot}1 < S \leqslant \beta$ ('strong' thermals), where Y is the fraction of the mass of the substance released which penetrated indefinitely into the lower layer. The constant β was approximately equal to 1·90.

In weak thermals, the equation $z - s = a_1(t - t_s)^2$ was obeyed while the front was in the lower layer, until the culminating point $z = s$ was reached at $t = t_s$. The acceleration a_1 was always negative, and constant for any one thermal, but varied between thermals. Also for weak thermals, $x = C_2 V^{\frac{1}{3}}/S$, where x is the distance from the interface to the culminating point and C_2 is a constant. C_2 was approximately equal to 3·5. For strong thermals, the distance travelled while the front was in the lower layer obeyed the equation $z^2 = k_2 t$. The origins of z and t usually differed from those found in the upper layer, and generally $k_2 \neq k_1$.

1. Introduction

In recent years, early attempts to describe the convection processes in the atmosphere which are responsible for the initiation and growth of cumulus clouds have led to 'bubble' and later 'thermal' models of buoyant convection (Bjerknes 1938; Stommel 1947; Davies & Taylor 1950; Scorer & Ludlam 1953; Scorer 1958).

In the experiments on the thermal model described by Scorer (1957), masses of marked salt solution were observed as they moved from rest at a free surface, under the action of buoyancy forces alone, into initially still water of uniform

* Now at Department of Electrical Engineering, Loughborough College of Technology.

density. It was seen that most of the marked fluid entered a well-defined region, or 'thermal', which moved through the surroundings in the direction of the buoyancy force. After an initial acceleration the shape of the thermal remained nearly constant, but its size increased continually and the rate of growth and speed of advance decreased continually.

In the experiments reported here, masses of opaque solutions were released at the surface of a comparatively shallow layer of water superimposed on a deep layer of sodium chloride solution of uniform density. As the lowest part of the thermal ('the front') approached the interface, the varying pressure distribution over the interface created waves, but the maximum displacement of the interface was always very small compared with any linear dimension of the thermal cloud while this remained entirely within the upper layer.

2. Motion in the upper layer

Dimensional analysis

The greatest linear dimension of every thermal was initally much less than the depth of the water layer, and we may therefore assume that the effect of the interface upon the early part of the motion was negligible. The accelerated part of the motion was brief, and will not be discussed. It will be assumed that the remainder of the motion may be sufficiently described by the following physical variables: the speed of advance of the front, dz/dt; the rate of increase of the maximum horizontal dimension of the thermal, $2dr/dt$; the total buoyancy force, Mg; the density of the surrounding fluid, ρ; and r. As usual, it is assumed that the fluid density may be taken as substantially equal to ρ everywhere except for the evaluation of buoyancy forces, and that the fluid viscosity is irrelevant to the motion.

A straightforward dimensional analysis then gives

$$r(dr/dt) = f_1(n_1)\,(Mg/\rho)^{\frac{1}{2}}, \tag{1}$$

where n_1 is defined by

$$dz/dt = n_1(dr/dt). \tag{2}$$

It was observed (see below) that n_1 was approximately constant only within experiments. Since Mg/ρ was also constant in each experiment, (1) indicates that $r(dr/dt)$ was constant within experiments. The Reynolds number $r(dr/dt)/\nu$ was therefore constant within experiments; and if the distribution of fluid velocities in each experiment is assumed to have been similar at all times, it follows that the circulation K round a circuit passing along the axis of an axisymmetric thermal and returning in the surrounding fluid, having the same dimensions as $r(dr/dt)$, was also constant within experiments. The dimensionless parameter $K^2\rho/Mg$ was therefore constant within experiments, but may be supposed to have varied between experiments as a result of variations in the initial conditions.

Vortex-ring model

A kinematic model of thermal motion has been advanced by Turner (1960). According to this model, a thermal may be regarded as a buoyant vortex ring having axisymmetric distributions of velocity and buoyancy. It is assumed that

these distributions are similar at all stages of the motion and that the circulation K, already defined, is constant within thermals. Turner showed that, for such a ring,

$$x_1 = (K^2\rho/Mg)\,mR, \tag{3}$$

where R is the radius of the circular axis of the vortex system (Lamb 1932, § 162), x_1 is the distance of the plane of the circular axis from a fixed virtual origin, and m is a dimensionless function of the vorticity distribution. Since, by the similarity assumption,

$$R = ar, \quad z = bx_1, \tag{4}$$

where a and b are constant within thermals, (3) may be written

$$z = abm(K^2\rho/Mg)\,r;$$

that is,

$$n_1 = abm(K^2\rho/Mg). \tag{5}$$

If the term abm is constant between thermals, this equation shows that n_1 is directly proportional to $(K^2\rho/Mg)$.

Experiments

Thermals having various mass excesses were released from a hemispherical cup. The cup was pivoted about a diametral axis which lay slightly above the free surface of the water in an experimental tank. This surface was initially coplanar with the surface of the fluid contained in the cup. Release was effected by rapidly inverting the cup about its fixed pivots.

The mass excess in the cup was found by measuring the volumes and densities of the solutions used. Standard gravimetric draining-error determinations showed that the mass excess released was always approximately 99 % of the mass excess in the cup. The corresponding values of $(z-z_0)$, $2r$ and $(t-t_0)$ were measured from enlarged images of cine photographs (z_0 is the vertical displacement of a fixed mark from the virtual origin $z = r = 0$, and $t = t_0$ at an arbitrary fixed instant). The separation of the images of two fixed marks at a known distance apart was measured to determine the scale of the photographic image. A graph of the observed values of $(z-z_0)$ was plotted against $2r$, and in each case a straight line fairly represented all except the earliest observations. The corresponding value of n_1 was found as twice the slope of this line (see (2)), and z_0 was determined as minus the intercept of the line on $2r = 0$.

From (1) and (2), we have

$$z^2 = k_1 t, \quad \text{where} \quad k_1 = f(n_1)\,(Mg/\rho)^{\frac{1}{2}}. \tag{6}$$

Graphs of z^2 against $(t-t_0)$ were plotted from the observations of each experiment. Straight lines fairly represented all except the earliest observations. This confirmed that the interface had little effect on the motion in the upper layer. The value of $f(n_1)$ for each experiment was found from the slope of the corresponding graph and the measured value of M, use being made of (6). The pair of graphs relating to one particular experiment are shown in figure 1.

Figure 2 shows a graph of the corresponding values of $f(n_1)$ and n_1 for each experiment. It will be seen that a wide range of values of n_1 was obtained, and that an equation of the form

$$f(n_1) = C_1 n_1^{\frac{3}{4}}, \quad \text{with} \quad C_1 = 0{\cdot}73, \tag{7}$$

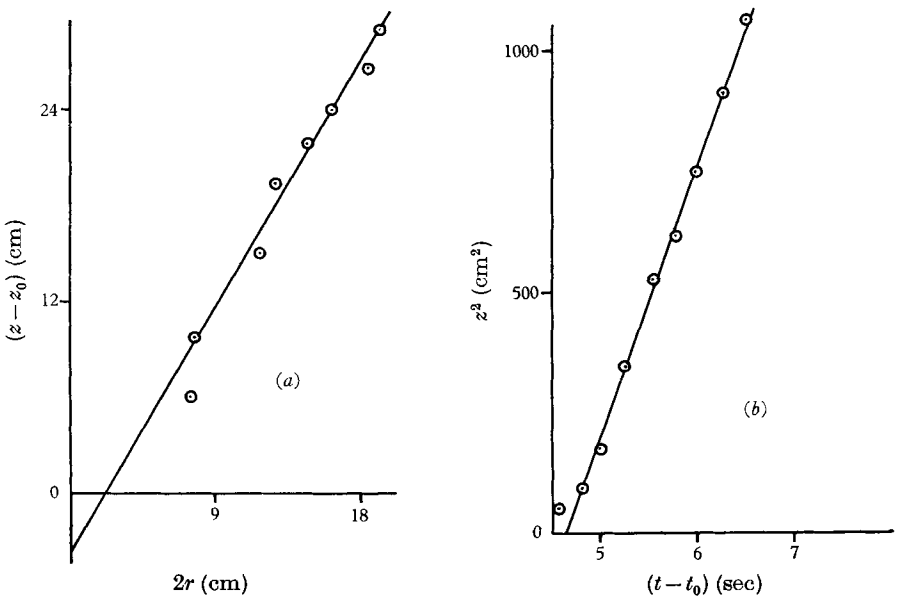

FIGURE 1. An example of motion in the upper layer.

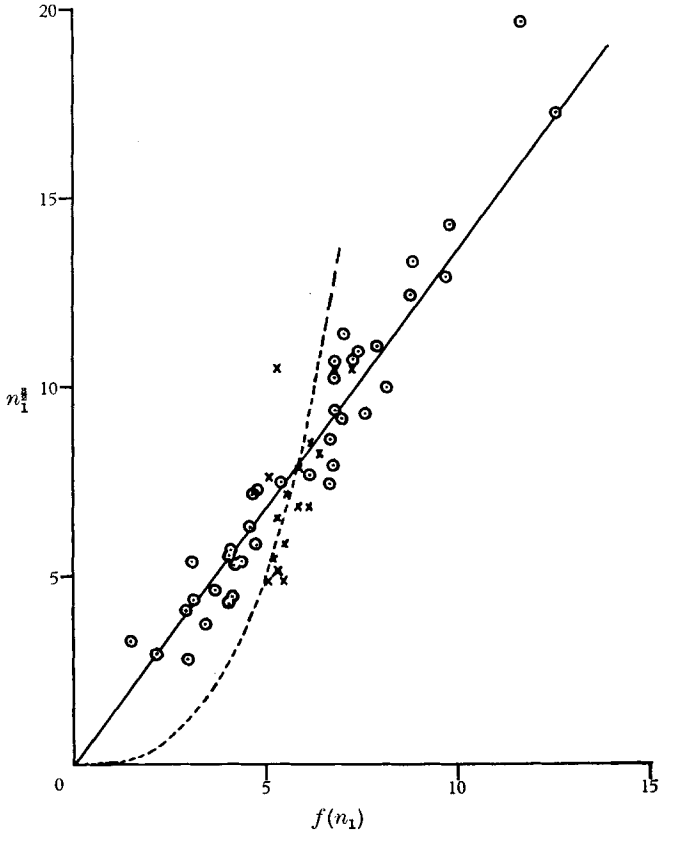

FIGURE 2. Relation between the angle of spread and rate of progress of thermals moving from a free surface into unstratified surroundings. The curve shown by the broken line is that suggested by Scorer (1957). ⊙, Richards; ×, Scorer.

fits the observations reasonably well. The value of C_1 was found as the reciprocal of the slope of the line in figure 2. Figure 2 also shows the observations reported by Scorer (1957). These are consistent with (7) and the present observations, but the latter are inconsistent with the empirical relation, $f(n_1) = 2{\cdot}9n_1^{\frac{1}{2}}$ (shown in figure 2 by a broken line) which was suggested in Scorer's paper.

Expt.	M (g)	$\Delta\rho$ (g/c.c. $\times 10^{-3}$)	V (l.)	Y	k_1 (cm^2/sec)	n_1	c	h (cm)
7	18·5	5·74	1·78	0·49	501	2·8	0·76	24
8	11·2	5·74	3·40	0·09	501	2·9	0·45	29
9	14·9	1·27	6·98	0·70	362	2·0	0·79	24
10	22·3	1·27	3·86	0·84	—	—	0·69	—
11	15·0	1·27	3·41	0·83	829	4·7	0·85	39
12	45·3	1·27	4·20	0·89	658	2·7	0·75	26
13	15·0	1·27	2·84	0·77	421	2·4	0·60	27
14	15·0	5·80	1·20	0·74	1085	5·6	0·60	41
15	11·3	5·80	1·19	—	714	4·8	0·84	37
16	15·2	5·80	2·68	0·77	912	4·9	0·78	41
21	15·1	3·92	3·03	0·60	496	2·6	0·72	27
22	15·1	3·84	4·23	0·38	756	3·9	0·87	35
23	15·1	3·65	1·66	0·67	1080	5·4	0·66	40
24	15·1	3·68	3·91	0·42	565	3·4	0·75	33
25	15·2	3·95	3·23	0·51	511	2·7	0·90	26
26	11·3	3·74	2·68	0·49	468	3·1	0·85	29
27	9·47	2·10	1·89	0·69	652	4·0	0·79	32
28	4·83	0·81	1·99	0·71	459	3·8	0·76	31
29	4·87	1·42	2·07	0·48	475	4·5	0·60	38
30	6·04	1·07	2·60	0·73	326	3·1	0·76	26
31	4·83	1·51	2·03	0·64	319	3·7	0·84	30
32	15·1	1·51	3·46	0·77	464	2·9	0·66	25
34	12·0	4·93	2·05	0·53	891	4·6	0·57	37
35	10·6	5·83	2·98	0·07	551	3·8	0·89	32
36	10·6	5·97	2·99	0·21	747	4·9	0·74	39
38	9·01	5·44	3·16	0·04	721	4·4	0·77	41
39	9·01	4·27	1·33	0·57	1048	7·3	0·63	45

TABLE 1. Measurements on strong thermals.

Note: c is the quotient (distance from level of widest part of thermal to virtual origin) ÷ (distance from front to virtual orgin).

It may be shown that the vortex-ring model leads to the equation

$$\pi z^2 = n_1^{\frac{3}{2}}(a^{-3}bm)^{\frac{1}{2}}(Mg/\rho)^{\frac{1}{2}}t. \tag{8}$$

This is consistent with (6) and (7) if $a^{-3}bm = (0{\cdot}73\pi)^2$ for all thermals. It is natural to suppose that the value of n_1 in each experiment is related to the manner of release. The controllable variables are the initial volume of the buoyant mass, the radius of the cup, and the speed with which the cup is overturned. The same cup (radius 2 in.) was used throughout. The density of the solution released was roughly 1·3 g/cm^3 in most experiments, so that the initial volume was roughly proportional to the mass excess for the experiment. However, according to the set of experimental results presented in table 1, there is no evidence of a relationship between the configuration at release and the corresponding value of n_1.

Preliminary trials showed that if the cup was inverted slowly, part of the fluid mass moved appreciably while part was still retained by the cup. The release then had the character of a pouring, and this tended to initiate plume-like rather than thermal motion. The release was so rapid in the main experiments that there was no visible distortion or descent of the buoyant mass while the cup was being overturned. However, the rate of overturning was not closely controlled or measured, and it is therefore possible that variations in this rate may have affected the value of n_1. In either case we should conclude that a wide variety of thermal motions may result from only slightly different initial circumstances.

3. Separation at the interface

The junction between the two layers of surrounding fluid was not strictly a discontinuity of density. However, we shall assume that the effect of the interface upon the thermal is determined only by the over-all difference in density between the layers, $\Delta\rho$. This assumption implies that, whenever any part of the thermal was being appreciably affected by the interface, a vertical dimension of the thermal should be large compared with the depth over which the density of the surroundings varied. This thermal thickness was at least four times the interface thickness in these experiments, so that the assumption seems reasonable.

If V_1 is the volume of the thermal as its front leaves the upper layer, the mean density excess in the thermal is then M/V_1. Material having this density excess would be neutrally buoyant in the lower layer if $M/V_1 = \Delta\rho$, that is if $V_1\Delta\rho/M = 1$. An increase in the parameter $V_1\Delta\rho/M$ therefore increases the difficulty with which a thermal may progress into the lower layer. If $V_1\Delta\rho/M$ is sufficiently great, the whole thermal will be buoyant in the lower layer, and must eventually return towards the interface. The magnitude of this critical value of $V_1\Delta\rho/M$ will depend on the rate at which the particular thermal entrains external fluid during its passage through the interface, and on the distribution of the intensity of this entrainment over the thermal surface. Some allowance for these factors will be obtained if the parameter is replaced by $V\Delta\rho/M$, where V is the volume of the thermal when its widest part is just leaving the upper layer. Let

$$V\Delta\rho/M = S. \tag{9}$$

Also let N_1 be the number of marked particles released, and let N_2 be the number which would still be moving downwards as $t \to \infty$ if the lower layer were of unlimited depth. Let

$$N_2/N_1 = Y, \tag{10}$$

where Y will be called 'the yield'. Evidently $Y = 1$ when $S = 0$, since the whole motion then takes place in unstratified surroundings. By the argument already given, $Y = 0$ for $S > \beta$, where β is a positive constant. We therefore distinguish two classes of thermals:

$$\left.\begin{aligned} &\text{'strong' thermals, for which } 0 \leqslant S \leqslant \beta \quad \text{and} \quad Y = F(S); \\ &\text{'weak' thermals, for which } S > \beta \quad \text{and} \quad Y = 0. \end{aligned}\right\} \tag{11}$$

The experiments were intended to determine the function F and the value of β.

Experimental method

The substance released was a solution of cobalt chloride in water, so that in our case N_1 was the number of cobalt ions released. The solution was strongly coloured, and visual and photographic observations were therefore possible without the use of added dyes.

After each experiment, the cobalt had become divided into two layers. The first layer was relatively shallow and was situated about the interface. This layer therefore contained $(N_1 - N_2)$ ions of cobalt. The second, deeper, layer rested on the bottom of the experimental tank, about 1·5 m below the interface. This layer, which contained the ions which would have penetrated indefinitely into an unbounded medium, was discarded by partly draining the tank. The remaining contents of the tank were stirred thoroughly so as to produce a homogeneous solution, the volume of this solution (about 320 l.) was found geometrically, and a number of 20 ml. samples were removed.

The concentration of cobalt in the samples was estimated by the method originally proposed by Haywood & Wood (1943) as modified by Eborall (1946). Briefly, the cobalt ions in the solution were caused to form a chemical complex by reaction with 'sodium nitroso-R salt' (sodium 1 nitroso 2 hydroxynaphthalene-3:6 disulphonate). The resulting substance, in weak solution, has an absorption coefficient for blue light which is directly proportional to its concentration. A measurement of the absorption over a known path length therefore gave the concentration of cobalt in the samples, and so the total amount of cobalt which had collected near the interface was determined. The method is not absolute, and the necessary calibration was carried out by mixing known small volumes of the stock solution of cobalt chloride into 320 l. of water, sampling and estimating the cobalt in the manner just described. The amount of cobalt remaining near the interface after an experiment was then expressed as a volume of the stock solution to which it was equivalent. This volume was divided by the volume of solution released to obtain the value of $(1 - Y)$ for the experiment.

Determination of $\Delta\rho$

The difference in density between the two layers was usually about 10^{-3} g/cm^3. A long uniform glass tube was partly filled with paraffin wax and weighted so as to weigh about 20 g when sealed at both ends and submerged in water. This sinker was suspended in the tank by two nylon monofilaments, one of which, attached near one end of the tube, was used to make the tube axis horizontal, as indicated by a spirit level fixed inside the tube. The other filament was attached near the middle of the tube and led to one arm of a balance. An application of the principle of moments determined what proportion of any change in the upthrust on the sinker would act on the filament attached to the balance. The tank contents being at rest, a change in the weight of the sinker was related, by Archimedes' principle, to a corresponding change in the 'mean density' of the surroundings. Terms of odd order in the distribution of density with depth did not affect the upthrust because the axis of the sinker was horizontal and the sinker was geometrically symmetrical about its axis. If any terms of even order are sufficiently small, the

mean density found from the upthrust approximates to the density at the level of the axis. This approximation was always sufficiently accurate in these experiments.

The sensitivity of the arrangement was 1 g change in balance for about 10^{-3} g/cm^3 change in density. The sinker was accordingly weighed at various depths, a typical graph of density change against depth being shown in figure 3. It will be seen that the interface was about 3 cm thick in this case.

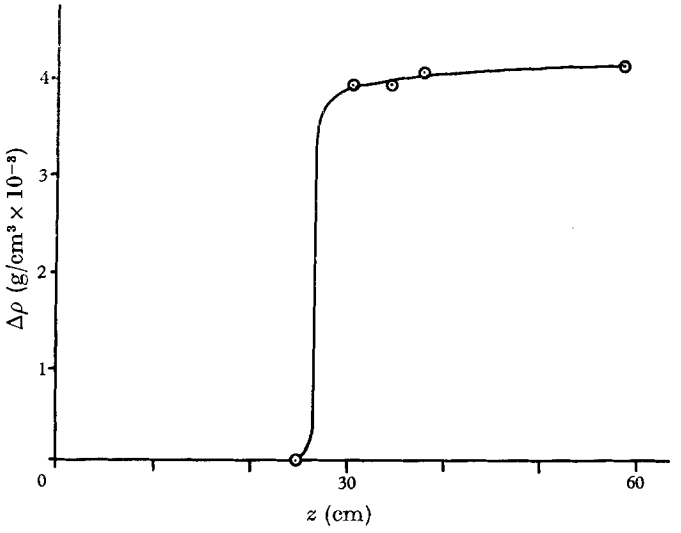

FIGURE 3. An example of the variation of the density of the surrounding fluid with depth. In the upper layer (low values of z) the density was constant. The lower layer had a slightly stable stratification.

Determination of V

Two cameras, so placed that their optic axes were respectively perpendicular to the front wall and to one of the side walls of the tank, made simultaneous exposures at the instant when the widest part of the thermal profile seen from the front of the tank was level with the top of the interface. Profile sketches like those shown in figure 4*a* were made from the enlarged images of these photographs. The profiles often indicated marked departures from axial symmetry.

With respect to the axes shown in figure 4*a*, Δx and Δy were measured at several levels z_1 in the thermal. Then V was found from the approximate expression

$$V \doteq \tfrac{1}{4}\pi \int (\Delta x\, \Delta y)\, dz_1. \tag{12}$$

The right-hand side of (12) was evaluated as $\frac{1}{4}\pi$ times the area under a graph such as figure 4*b*. Equation (12) is accurate in the case of axial symmetry, and may be accurate, depending on the orientation of axes, when horizontal cross-sections of the thermal are elliptical.

Experimental results

The graph of Y against S is given in figure 5, which shows that Y varies roughly linearly with S over a certain range. The slope of the line is approximately $-0{\cdot}5$. The results in figure 5 and table 2 may be expressed in the form

$$\left.\begin{aligned} Y &= 0{\cdot}95 - \tfrac{1}{2}S \quad \text{when} \quad 0{\cdot}1 < S \leqslant 1{\cdot}9, \\ Y &= 0 \qquad\qquad\ \text{when} \qquad\quad S > 1{\cdot}9. \end{aligned}\right\} \tag{13}$$

Additionally, we know that $Y = 1$ at $S = 0$, but the experiments have not revealed the relation between Y and S in the range $0 < S \leqslant 0{\cdot}1$.

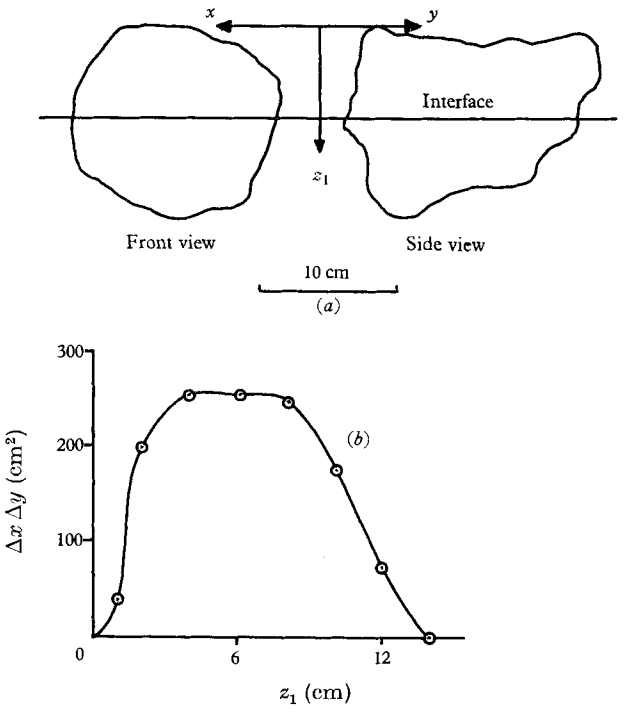

FIGURE 4. (*a*) Simultaneous profiles of a typical thermal. (*b*) Graphical determination of the thermal volume V (Δx and Δy are the widths across the profiles at the level z_1).

Now, S is not the only dimensionless parameter which can be constructed from the conditions of the experiments. For example, $h/V^{\frac{1}{3}}$ is another such parameter, where h is the vertical distance of the interface from the virtual origin of the thermal motion. Although $h/V^{\frac{1}{3}}$ varied between 1·0 and 4·1 in these experiments, the variations appear to have had no significant effect upon Y.

4. Motion in the lower layer: weak thermals

In this case there is a lower limit to the progress of any part of the thermal mass. Outline sketches of a typical weak thermal at successive instants are shown in figure 6. The distance z of the front from the virtual origin of motion in the upper

layer increases to a maximum (at the 'culminating point') and then decreases. Let s be the value of z, and t_s the value of t, at the culminating point. It was found that, for every weak thermal when $t < t_s$, the graph of $(z-s)$ against $(t-t_s)^2$ was a straight line in the lower layer. An example is shown in figure 7.

This was motion with a constant deceleration, such as might be expected when a parcel of fluid moves through uniform surroundings in the direction opposed to that of the buoyancy force. Since mixing at the front between the parcel and its

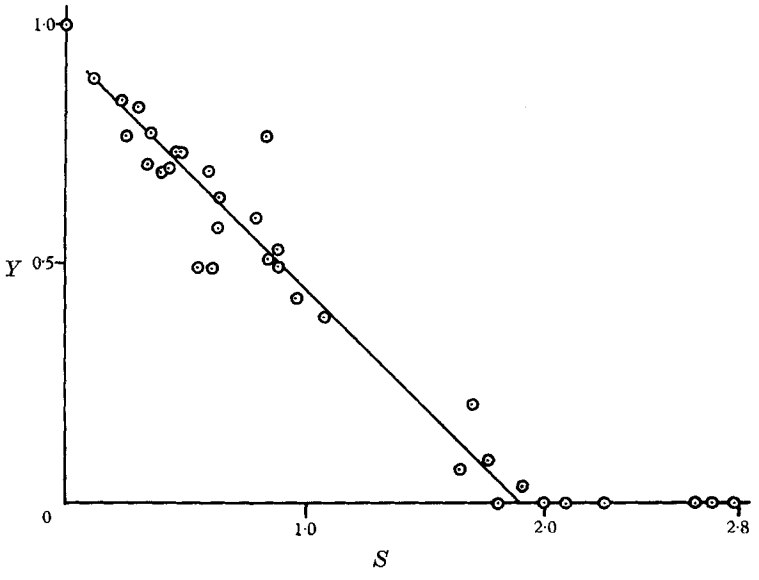

FIGURE 5. Relation between the fraction of the mass released which penetrated the inversion and the relative strength of the thermal.

Expt.	M (g)	$\Delta\rho$ (g/c.c. $\times 10^{-3}$)	V (l.)	k_1 (cm²/sec)	n_1	x (cm)	h (cm)	a_1 (cm/sec²)	v_2/v_1
6	8·07	5·62	3·79	594	4·2	16·5	31	0·66	0·48
17	11·4	5·89	4·01	505	3·8	31·3	33	0·32	0·59
51	1·05	1·64	5·72	224	4·4	8·8	39	0·15	0·58
52	2·10	1·64	2·84	572	6·7	16·4	57	0·21	0·53
53	3·10	1·62	3·78	223	3·1	25·3	29	0·14	0·73
54	2·48	1·62	4·98	154	3·1	16·6	30	0·17	0·92
55	0·64	1·69	4·36	74	2·6	4·7	24	0·14	0·73
56	1·48	1·69	3·81	304	5·0	17·2	38	0·29	0·80
57	1·25	4·12	2·20	248	5·1	7·9	36	0·42	0·74
58	2·89	4·12	2·30	—	—	12·9	—	0·66	—
59	4·08	4·01	1·81	624	5·9	27·2	39	0·23	0·60
60	6·66	4·01	4·32	121	2·2	20·9	16	0·58	1·28
61	4·16	4·29	4·29	138	2·1	9·9	20	0·69	1·06
62	6·22	4·29	3·98	760	5·5	22·9	46	0·35	0·48

TABLE 2. Measurements on weak thermals ($Y = 0$).

Note: x is the distance from the interface to the culminating point.

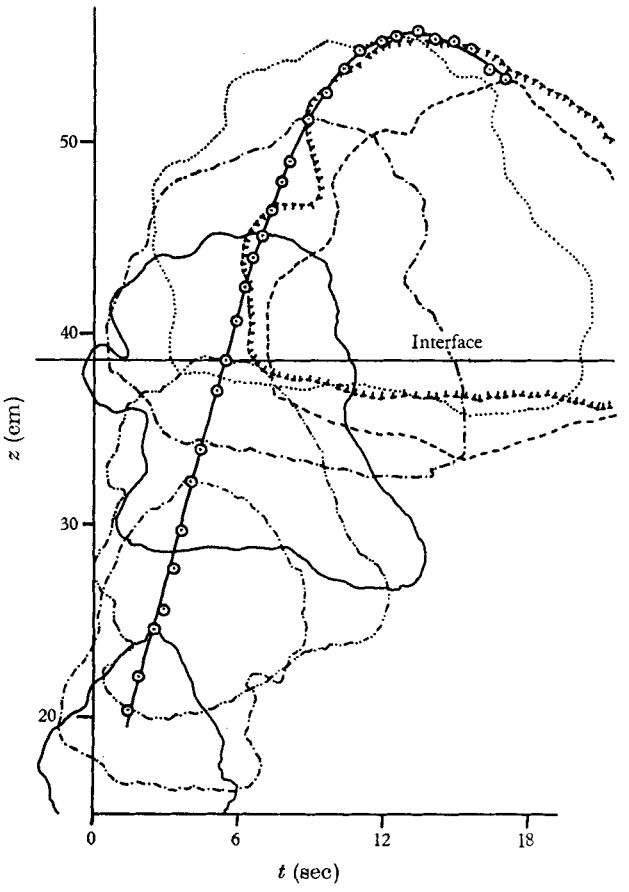

FIGURE 6. The motion of a weak thermal above and below an interface. The solid curve shows the (z, t)-variation, and the other symbols distinguish the successive thermal profiles. Low values of z refer to the upper layer.

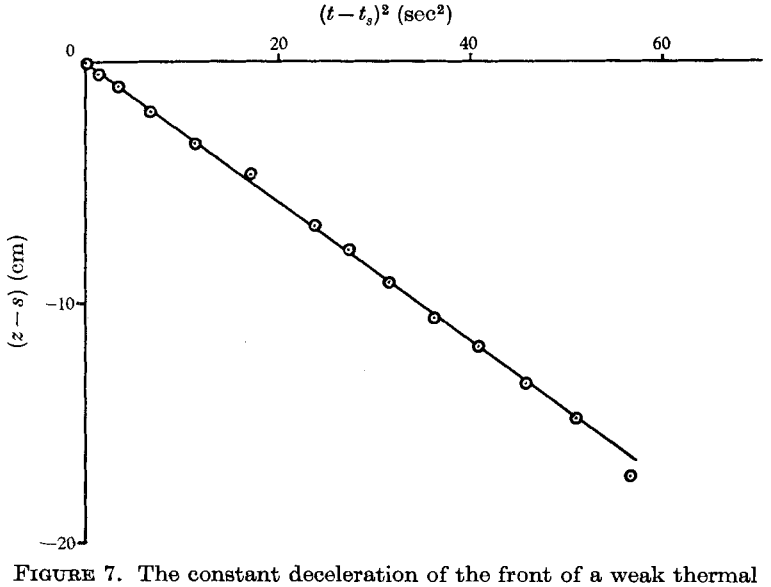

FIGURE 7. The constant deceleration of the front of a weak thermal while in the lower layer.

surroundings then has the effect of working more rapidly against the buoyancy force, the intensity of such mixture may be expected to decrease rapidly as the thermal moves into the lower layer.

In the lower layer,

$$z - s = a_1(t - t_s)^2. \tag{14}$$

Accordingly, let x be the distance from the interface to the culminating point. If (14) held near the interface, the velocity of the front at the interface would be

$$v_2 = \sqrt{(-2a_1 x)}, \tag{15}$$

which will be called the 'virtual velocity'. But, from (6), the actual velocity of the front at the interface is

$$v_1 = k_1/2h, \tag{16}$$

since $z = h$ at the interface.

It will now be assumed that the particle of fluid which is at the front when the weak thermal touches the interface remains at the front until the culminating point is reached, and that there is no mixture between other fluid and this particle while it is in the lower layer.

The density difference between the particle and its environment, which consists largely of fluid of the lower layer, is

$$(K_1 M/V) - \Delta\rho, \tag{17}$$

where K_1 is a numerical constant.

The kinetic energy per unit volume of the particle is some fraction of the average potential energy per unit volume given up by the thermal in its progress from the virtual origin to the interface. The kinetic energy per unit volume of the particle at the interface is therefore

$$C_2 V^{\frac{1}{3}} Mg/V, \tag{18}$$

where C_2 is a numerical constant. If the energy which the particle gains while in the lower layer is negligible, the kinetic energy density (18) is equal to the potential energy density of the particle at the culminating point, so that

$$-\{(K_1 M/V) - \Delta\rho\} gx = C_2 V^{\frac{1}{3}} Mg/V.$$

That is,

$$V^{\frac{1}{3}}/x = (S - K_1)/C_2. \tag{19}$$

Experimental results

These are shown in table 2. The value of a_1 was determined as the slope of the corresponding graph like figure 7, x was measured directly from the photographic images, and v_2 and v_1 were calculated from (15) and (16).

It will be noticed that v_2/v_1 varied between 0·48 and 1·28. This seems consistent with Miss Woodward's observation (1959) that the maximum mean vertical component of the fluid velocity in a thermal moving through unstratified surroundings is about twice the velocity of the thermal front.

The experimental values of $V^{\frac{1}{3}}/x$ have been plotted against S in figure 8, for both strong and weak thermals. It will be noticed that there is a sharp break, corresponding to the division between strong and weak thermals, near $S = 1{\cdot}9$. In the weak-thermal region, to the right of this break, a roughly linear relationship is

evident. If the line were produced, it would pass through or near the origin, and $V^{\frac{1}{3}}/x$ is therefore roughly directly proportional to S. This is the form taken by (19) if K_1 is much less than the minimum value of S which is possible in weak thermals, namely $S = 1{\cdot}9$. The value of C_2, obtained from the slope of the graph in figure 8, is 3·6.

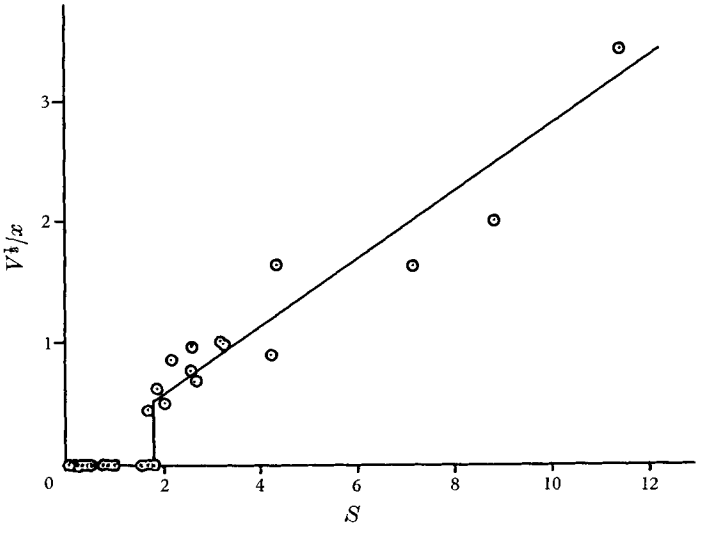

FIGURE 8. The penetration of an interface by thermals. Points to the left and right of the step represent strong and weak thermals respectively.

5. Motion in the lower layer: strong thermals

Substantially all that part of a strong thermal which would proceed indefinitely into the lower layer is denser than the surrounding fluid. If the advancing part had not been stopped, the momentum which it had on leaving the interface would eventually have become a small fraction of the total momentum, which would have been continually augmented by the action of the buoyancy force. It therefore seemed possible to suppose that thermal motion might be resumed in the lower layer at a sufficient distance below the interface.

This motion would be described by the equations

$$z = n_2 r, \tag{20}$$

$$z^2 = k_2 t, \quad \text{where} \quad k_2 = C_1 n_2^{\frac{3}{2}} (M_2 g/\rho_2)^{\frac{1}{2}}. \tag{21}$$

Equations (2), (6) and (7) have been used with a suffix 2 to refer to variables in the lower layer. C_1 would have the value obtained from the experiments in the upper layer.

Experiments

The observations in each experiment were reduced to graphs of $(z - z_0)$ against $2r$ and of z^2 against t. Typical results are shown in figures 9 and 10. In both these experiments it will be seen that $z = n_2 r$ throughout the motion in the lower layer, verifying (20). In most experiments, however, r seemed to be nearly constant in the earliest part of the motion in the lower layer, while the advancing part was

separating from the remainder of the marked fluid. The first equation of (21) was always approximately obeyed in the lower layer, typical cases being shown in figures 9*b* and 10*b*. It is therefore reasonable to suppose that (20) was also always approximately obeyed, but that the lateral extent of the advancing part was

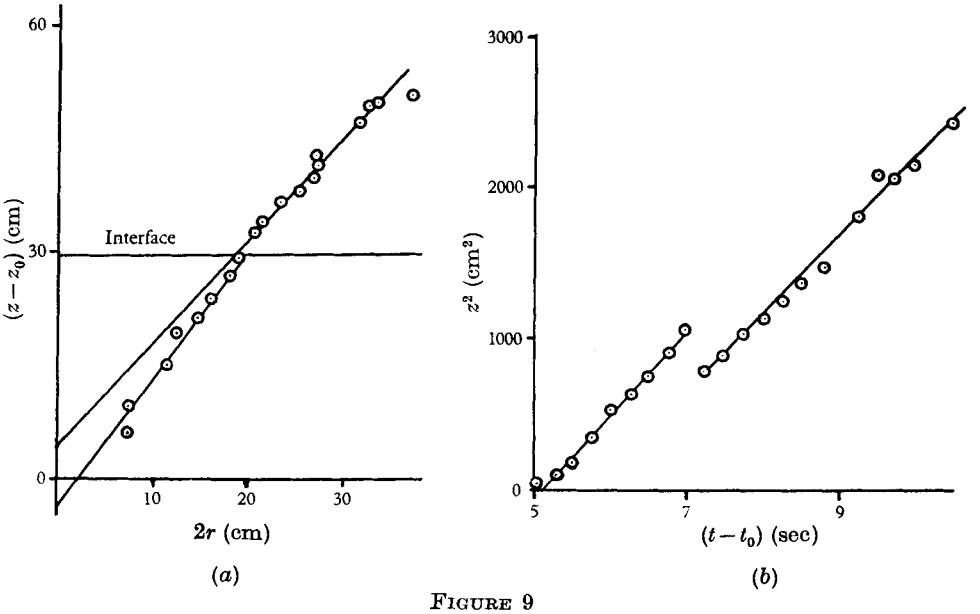

FIGURE 9

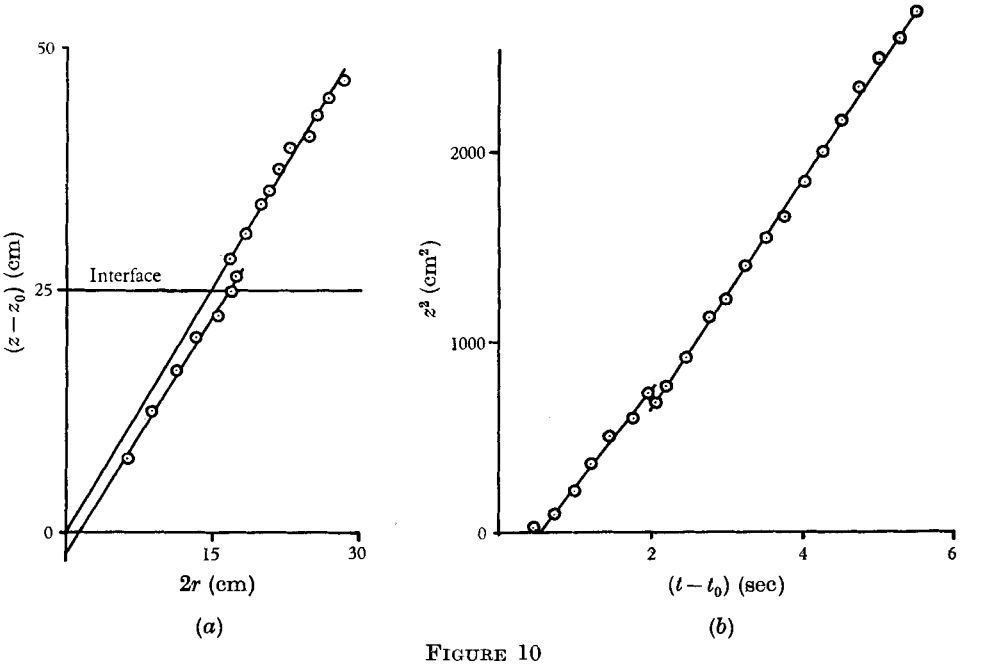

FIGURE 10

FIGURES 9 and 10. The motions of two strong thermals above and below an interface.

obscured by the remainder for a varying interval. In some cases this transitional behaviour persisted throughout the observed motion in the lower layer, so that no estimate of n_2 could be obtained.

From (6), (7) and (21), if thermal motion is resumed in the lower layer, we have

$$k_2 n_1^{\frac{3}{2}}/k_1 n_2^{\frac{3}{2}} = (M_2/M)^{\frac{1}{2}}, \tag{22}$$

since $\rho \doteqdot \rho_2$ in all experiments. The mass excess in the lower layer was always less than M since, first, the yield was always less than unity, and secondly, the surrounding fluid in the lower layer was always denser than that in the upper, so that the mass displaced by the advancing part of the thermal was increased and its mass excess therefore reduced. Hence, if thermal motion is resumed in the lower layer,

$$k_2 n_1^{\frac{3}{2}}/k_1 n_2^{\frac{3}{2}} < 1. \tag{23}$$

The experimental values of $k_2 n_1^{\frac{3}{2}}/k_1 n_2^{\frac{3}{2}}$ are shown in table 3, where it will be seen that about half these values are greater than unity.

Expt.	k_2 (cm²/sec)	n_2	$k_2 n_1^{\frac{3}{2}}/k_1 n_2^{\frac{3}{2}}$	Expt.	k_2 (cm²/sec)	n_2	$k_2 n_1^{\frac{3}{2}}/k_1 n_2^{\frac{3}{2}}$
7	584	3·6	0·81	26	283	1·7	1·41
8	680	4·1	0·79	27	708	—	—
9	531	—	—	28	459	3·8	1·00
11	958	4·7	1·15	29	319	—	—
12	1238	3·4	1·23	30	382	3·1	1·17
13	704	—	—	31	447	4·2	1·19
14	710	4·2	0·99	32	613	3·4	1·15
16	551	3·0	1·44	34	576	4·6	0·65
21	720	—	—	35	282	2·3	1·13
22	499	3·1	0·92	36	412	3·4	0·93
23	834	4·1	1·15	38	388	3·2	0·93
24	527	2·7	1·31	39	270	2·1	1·68
25	331	2·3	0·87				

TABLE 3. Comparison of motions above and below an interface (strong thermals).

We conclude that the motion of the advancing part of a strong thermal differs from thermal motion from rest at a horizontal surface into unstratified fluid. Returning to the vortex-ring model, we see from (8) that values of $k_2 n_1^{\frac{3}{2}}/k_1 n_2^{\frac{3}{2}}$ greater than unity may occur if, and only if, the value of $a^{-3}bm$ is sufficiently increased by the passage through the interface. This means that, according to the vortex-ring model, the distributions of velocity are sometimes necessarily different in the two layers.

I wish to thank Dr R. S. Scorer for many helpful discussions and Professor P. A. Sheppard for the use of experimental facilities, also Dr J. F. Herringshaw for advice and the use of apparatus and Mr S. J. Farnsworth for assistance in the determination of draining errors. My thanks are further due to Mr E. G. Jennings and his staff for workshop assistance, and to the D.S.I.R. for financial provision for this research and for permission to publish the results.

REFERENCES

BJERKNES, J. 1938 *Quart. J. Roy. Met. Soc.* **64**, 325.
DAVIES, R. M. & TAYLOR, G. I. 1950 *Proc. Roy. Soc.* A, **200**, 375.
EBORALL, F. E. 1946 *Metallurgia*, **39**, 104.
HAYWOOD, F. W. & WOOD, A. A. R. 1943 *J. Soc. Chem. Ind.* **62**, 37.
LAMB, H. 1932 *Hydrodynamics*, 6th ed. Cambridge University Press.
SCORER, R. S. 1957 *J. Fluid Mech.* **2**, 583.
SCORER, R. S. 1958 *Natural Aerodynamics.* London: Pergamon.
SCORER, R. S. & LUDLAM, F. H. 1953 *Quart. J. Roy. Met. Soc.* **79**, 94.
STOMMEL, H. 1947 *J. Met.* **4**, 91.
TURNER, J. S. 1960 *J. Fluid Mech.* **7**, 419.
WOODWARD, B. 1959 *Quart. J. Roy. Met. Soc.* **85**, 144.